Surface mining identification and ecological restoration effects assessment using remote sensing method in Yangtze River watershed, China

Suchen Xu
Zhejiang University
Kechao Wang (kechaowang@zju.edu.cn)
Zhejiang University https://orcid.org/0000-0002-2713-3810
Wu Xiao
Zhejiang University https://orcid.org/0000-0003-2493-0694
Tong Tong
Zhejiang University
Hao Sun
China University of Mining and Technology
Chong Li
China CMAC Engineering CO., LTD

Research Article

Keywords: Surface mining, Yangtze River watershed, Ecological restoration, Remote sensing ecological index, Google Earth Engine (GEE)

Posted Date: November 7th, 2023

DOI: https://doi.org/10.21203/rs.3.rs-3419136/v1

Abstract

Mineral resource development is necessary for economic growth, but its negative impacts on land, ecology, and the environment are significant and cannot be ignored. Identification the mine restoration process in a large scale is challenging without specific mining location information. Besides, how to quantitatively evaluates the ecological restoration effects became important for management and supervision. Here, we propose a systematic workflow that utilizes open-source remote sensing data to identify and assess large-scale surface mining areas' restoration status and ecological quality without prior knowledge of mine locations, and implemented in Yangtze River region, the largest watershed area in China. The process includes: (1) extracting surface mining areas using masking, morphological operations, and visual interpretation techniques; (2) constructing time-series of Bare Surface Percentage (BSP) for each mining area on the Google Earth Engine platform to distinguish between abandoned and active mines and examine their restoration rates; (3) constructing the Remote sensing Ecological indicator for Mining areas (REM) to quantify ecological quality and its temporal changes. The results show that: (1) the proposed method effectively identifies surface mining areas with higher boundary delineation accuracy and smaller omission numbers; (2) a total 1,183 mine sites were identified in the study area, of which 381 abandoned mines showed a significant decreasing trend in BSP from 2016 to 2021, with a median decreasing from 98% in 2016 to 81% in 2022, indicating better vegetation recovery during this period. (3) the REM of abandoned mines generally showed a stable upward trend from 2016 to 2022, and vice versa. This study provides a systematic solution for identifying surface mining areas and monitoring restoration scope and ecological quality on a broader scale. It can be extended to other areas and support further ecological restoration decision-making.

1. Introduction

As the wave of industrialization sweeps across the globe, countries are entering into a period of growth in industrial mineral resource consumption, achieving rapid accumulation of social wealth through the extensive consumption of natural resources. Studies have shown that 51% of mining areas are concentrated in five countries, namely China, Australia, the United States, Russia, and Chile (Maus et al., 2020). As the world's largest consumer of coal, aluminum and rare earth elements, China's consumption accounts for approximately 50%, 56% and 90% of the global total by 2020, respectively (Li et al., 2022). Mineral resources are one of the important material bases that support social development and play an important role in various production fields.. Surface mining, as one of the mining methods, removes large amounts of vegetation and soil from the surface, leaving solid waste accumulates on the surface, causing greater ecological damage than underground mining (Xiao et al., 2023). In addition, if follow-up ecological restoration is not timely and effective, it can cause long-term damage to the soil (Ahirwal and Maiti, 2016), vegetation (Huang et al., 2015; Ren et al., 2022), landscape (Karan et al., 2016), and groundwater (Xiao et al., 2020; Xing et al., 2018) in the local and surrounding areas. Therefore, governments have introduced mining regulations and reclamation laws, and more and more domestic

and foreign scholars have begun to pay attention to mining area identification and extraction, restoration effect monitoring, and mining area environment assessment.

Existing monitoring and ecological assessments of open-pit mine restoration are often conducted with known mine location information (Han et al., 2021). The lack of accurate mining spatial information is a crucial issue that hinders the monitoring of large-scale mines (Xiao et al., 2023).. Existing methods for extracting mining area location and boundaries can be roughly divided into three categories: field surveys (Zhang et al., 2021), visual interpretation of remote sensing images (J. X. Xu et al., 2018), and automatic classification algorithms for land use changes (Wu et al., 2018). Traditional field survey methods rely on a large amount of auxiliary data and field work to determine the mining area location and evaluate restoration effects. However, this method is costly, and measurement data may be subject to human errors, resulting in low efficiency, slow progress, and high costs (Zhang et al., 2021). In recent years, remote sensing technology has provided a new solution for extracting mining area location (Yang et al., 2018). The operation of sensor platforms such as MODIS, Landsat, and SPOT has made it possible to obtain images with larger spatial and temporal resolutions, accumulating massive multi-source, multi-resolution, and multi-scale remote sensing data (Zhang et al., 2021). Moreover, an increasing number of remote sensing cloud computing platforms, such as Google Earth Engine (GEE) (Gorelick et al., 2017), have greatly simplified the remote sensing experiment process by providing online remote sensing data operation, and have been widely applied by researchers in processing large amounts of data and algorithms (Tamiminia et al., 2020). On the basis of the aforementioned software and hardware, visual interpretation of satellite images (Werner et al., 2019) has been applied to draw maps of 295 mines around the world that are most relevant to primary commodity production (Murguía and Bringezu, 2016; Werner et al., 2020). However, visual interpretation over large areas is costly, not only involving huge workload but also subjective judgments by workers leading to errors (Maus et al., 2020). In addition, with the continuous improvement of computing infrastructure performance, many studies apply automatic classification algorithms (Belgiu and Drăguţ, 2016; Mountrakis et al., 2011; Zhu et al., 2017, 2019) to monitor land use changes for extracting mining area location and boundaries in many regions (LaJeunesse Connette et al., 2016; Mukherjee et al., 2019; Petropoulos et al., 2013; Vasuki et al., 2019; Yu et al., 2018). For example, recent research progress attempts to apply time series analysis to mining areas to achieve the goal of long-term monitoring and data reconstruction of mining disturbance (Lechner et al., 2016; Li et al., 2015). However, automatic classification algorithms rely on a large number of labeled examples (Mitchell Waldrop, 2019), and extending automatic classification algorithms to research areas of larger scales is difficult due to the heterogeneity between regions (Maus et al., 2020).

Many other studies have described various measurement and calculation methods to quantify and determine the restoration effect and ecological quality of mining areas. For example, the effect of farmland reclamation can be determined by soil data since the saturated hydraulic conductivity and bulk density of soil can reflect soil productivity (He et al., 2020; Zhang et al., 2022). However, soil data is dependent on field sampling, which on one hand, requires high costs, and on the other hand, cannot reflect the temporal and spatial changes of the ecological quality of mining areas (Xiao et al., 2022). The development of remote sensing technology provides technical support for timely and accurate monitoring

of the ecological and environmental conditions of mining areas and the progress of restoration projects, making it easier to monitor long-term conditions (Xiao et al., 2023). For example, Wang et al. (2019) used multi-temporal remote sensing images and the decision tree algorithm to identify the characteristics of the coal mining process and the disturbance to surface vegetation in the past 34 years (Zhang et al., 2021). Multiple ecological indicators from remote sensing data, such as the Normalized Difference Vegetation Index (NDVI), Standardized Precipitation Index (SPI), Land Surface Temperature (LST), and Ratio Drought Index (RDI), have been applied to measure ecological-environmental quality (Singh et al., 2017; Zarch et al., 2015). Among them, NDVI has been confirmed by a series of studies as a competent index for monitoring vegetation in mining areas (Xiao et al., 2021) (Du et al., 2018; Yang et al., 2018) and can be used to quantitatively assess the effectiveness of mine restoration. Various restoration methods in surface mining areas have different impacts on ecosystem elements, including soil, heat, water, and vegetation (Zhang et al., 2022). Specifically, soil elements are reflected in soil moisture, structure, and texture (He et al., 2020); thermal elements are reflected in local heat island effects and temperature distribution; water elements are reflected in local water resource allocation (Demetriou et al., 2012); and vegetation elements are reflected in local vegetation quantity structure and spatial pattern (Sklenicka et al., 2014). Therefore, indicators such as humidity, greenness, heat, and dryness can be incorporated into the Remote Sensing Ecological Index (RSEI) to represent the response of ecological-environmental elements brought on by restoration (H. Q. Xu et al., 2018). However, although RSEI is a more reliable remote sensing ecological indicator than many other indicators such as the Ecological Index (EI), it fails to effectively take into account the differences between bare soil and bare rock in sparsely vegetated areas and the differences in ecological quality due to plant diversity in densely vegetated areas when applied to mining scenarios (Xiong et al., 2021; Xu et al., 2019).

The restoration and management of abandoned mining areas have become a focal point for governments and scholars worldwide, with particular attention given to ecological restoration of abandoned mines. Since the early 20th century, countries such as the United States, Germany, Canada, and Australia have enacted relevant laws and regulations (Zhang et al., 2021). Under the overall requirements of building an ecological civilization in China, mining governance has also received high attention. The Mineral Resources Law and the Ecological Restoration Work Plan for Abandoned Open-pit Mines in the Yangtze River Economic Belt were formulated to regulate mining activities. However, the Yangtze River Economic Belt, as a major national development strategy area, has highly overlapping ecological functional areas and mineral resource ore belts in space, resulting in severe damage to the ecosystem during the process of mineral resource development. Mining activities have caused water pollution, heavy metal pollution, and risks of geological disasters, which have posed significant threats to human settlements (Zhang et al., 2021).

In order to achieve sustainable development and promote the complementary relationship between ecological protection and high-quality economic development, China carried out the restoration of abandoned open-pit mines within a range of 10 km along the main and tributary rivers of the Yangtze River from 2016 to 2020. This work required the establishment of archives for abandoned mines in the region, restoration of vegetation, and reduction of bare land. However, traditional field survey methods for

determining mining locations and evaluating restoration effectiveness are costly, subjective, and time-consuming, requiring significant amounts of auxiliary data, visual interpretation, and fieldwork. Furthermore, current automatic classification algorithms are not suitable for the large-scale extraction and restoration evaluation of open-pit mines in the Yangtze River Economic Belt, and existing remote sensing indices have not adequately accounted for the differences between sparse and dense vegetation areas. There is a lack of an automated, efficient method for extracting mining areas, and quantitative research on monitoring and evaluating ecological restoration in open-pit mines is also insufficient. Therefore, this study aims to address two main issues: (1) how to obtain the distribution of mining areas within a region and (2) how to evaluate the effectiveness of restoration projects. To achieve economic, objective, and fast mining area location extraction and restoration evaluation, this study used the Google Earth Engine (GEE) cloud platform to interpret and delineate mining area boundaries based on spectral-temporal characteristics and morphology operations using high-resolution remote sensing images and Sentinel-2 data. In addition, vegetation indices (NDVI), surface bareness proportion (BSP), and remote sensing integrated ecological index (REM) were used to evaluate the restoration effectiveness and environment quality of mining areas. This study provides insights that may assist research on mining restoration and governance in countries worldwide.

2. Material and methods

2.1 Research area and data

2.1.1 Research area

The Yangtze River Economic Belts is one of China's most important strategic development areas, which spans China's three elevation gradients from east to west, covering 11 provinces including Shanghai, Jiangsu, and Zhejiang (Fig. 1). It has an area of 2.05 million km^2, making up 21.4% of the nation. It is not only the location of the core area of China's economic development, but also a pioneering demonstration zone for the nation's eco-civilization construction, with extremely abundant freshwater resources and a wide variety of mineral resources with large reserves along the streams. Given its unique geographical location and development potential, mining in the Yangtze River basin along the main stream and tributaries is progressing rapidly and on a large scale. However, as mining continues, the environment of the Yangtze River Basin begins to face great threats. Specifically, the abandoned open-pit mines in Yunnan, Guizhou, Sichuan, and Chongqing are mainly iron, manganese, and rare earths, and geological disasters such as landslides and mudslides are relatively frequent. The abandoned open-pit mines in Jiangxi and Hunan are dominated by non-ferrous metals and rare earths, while in Hubei they are dominated by phosphate mines, and the problems of heavy metal water and soil pollution are prominent. The abandoned open-pit mines in Anhui are dominated by metals such as iron and copper and non-metals such as limestone, while those in Jiangsu, Zhejiang, and Shanghai are dominated by building materials mines, and the problems of mountain and vegetation damage are serious. Based on this status, China carried out the ecological restoration of open-pit mines within 10 km on both sides of the main

streams and tributaries of the Yangtze River from 2016 to 2020, and completed the restoration and acceptance in 2020. However, there are a large number of open-pit mines along the streams with strong heterogeneity. Under the traditional methods, the identification of mining areas and the evaluation of mine restoration effects require a lot of visual interpretation and field work, and also requires a lot of economic and time cost, and the subjectivity of the evaluation is too strong, which is not conducive to the development of mine restoration and governance research. Therefore, it is necessary to establish an objective, economical, and rapid implementation method for surface mining identification and restoration effect monitoring, so as to promote the sustainable research and effect evaluation of ecological restoration in mining areas.

2.1.2 Data

The data used in this study include: Yangtze River linear feature data, built-up area distribution data, Yangtze River Basin Sentinel-2 remote sensing image data, water body distribution data, vegetation distribution data and snow distribution data. Among them, the latter two are computationally extracted from the Sentinel-2 remote sensing image data of the Yangtze River Basin.

The Yangtze River linear feature data was downloaded from the Chinese Academy of Sciences Environmental Resources Data Sharing Platform, and the specific stem and tributary information included the main stem (6397 km) and seven major tributaries of the Han River (1577 km), Jialing River (1120 km), Min River (735 km), Yalong River (1637 km), Wu River (1037 km), Xiang River (844 km) and Gan River (766 km). The data of the built-up area were obtained using the 2019 annual China Land Cover Dataset (CLCD) product constructed by the R&D team of Wuhan University (Fig. 2). The water distribution data was adopted from the JRC monthly water history dataset v1.3 developed by the Joint Research Center of the European Commission, which had a resolution of 30 m and contained the spatiotemporal distribution of water surfaces and related statistics from 1984 to 2022 on a global scale. Remote sensing data of the Yangtze River basin were obtained using Sentinel-2 remote sensing images from June to September of each year from 2016 to 2022, and vegetation distribution data and snow distribution data were extracted from the 2016 remote sensing images. The specific data types and sources are shown in Table 1.

Table 1
Data type and sources

Data	Type	Resolution	Source
Sentinel-2 images	Raster	10m	https://sentinel.esa.int/web/sentinel/
China Land Cover Dataset (CLCD)	Vector	/	https://zenodo.org/record/4417810#.YmOo5YVBxPY
JRC Global Surface Data	Raster	30m	https://global-surface-water.appspot.com/
The Yangtze River linear feature data	Vector	/	https://www.resdc.cn/

2.1.3 Analysis framework

The data analysis of this study was mainly completed on the Google Earth Engine (GEE) platform, and the cartographic expression of the results was carried out in ArcGIS software. This work mainly includes three parts: identification of surface mining areas, monitoring of restoration and evaluation of the environment, respectively (Fig. 2). First is surface mining areas identification. We imported the linear object data of the Yangtze River on the GEE platform and constructed a 10-km buffer zone, and masked the study area with the processed water body data, vegetation data, built-up area data and snow data to remove irrelevant land types, which greatly reduced the study area. To solve the interference of the salt and pepper phenomenon (mainly rural residential areas) in the masked image, we eliminated isolated pixels through morphological operations. Among the remaining features, we referred to the interpreted signs of the mining area to interpret the mine spots and outline and digitize the boundaries of the mining area. In the second step, in order to detect the restoration of the mining area, we constructed the indicator of the Bare Surface Percentage (BSP) to judge the restoration according to the reduction of the bare land area. Mann-Kendall Test was performed on the BSP time series of individual mining area to determine whether the time series has a monotonic trend and whether it is statistically significant, and to distinguish abandoned mining areas from non-abandoned mining areas. On this basis, the overall restoration rates of the upper, middle and lower reaches of the study area were further calculated. Finally, the study evaluated the ecological conditions of the study area. A time series of ecological status indicators was constructed and the change results were analyzed. In this study, the remote sensing ecological index for the study area was constructed according to the REM index proposed by Sun (2022).

2.2 Methodology

2.2.1 Remote sensing identification and digitization of surface mining areas

In order to objectively, economically and quickly identify surface mining areas within 10 km along the Yangtze River, this study developed a set of " Mask irrelevant land class - Remove isolated pixels - Visual interpretation of mine boundaries" workflow based on Sentinel-2 images of the Yangtze River Basin (Fig. 4), to maximize the efficiency and accuracy of identification and reduce its cost.

Since the study area reaches 132633.9 km^2 large, even after removing the built-up area, the area is still 126,148 km^2, it was not conducive to direct mining extraction. Considering that the snow area, water body area, and vegetation area vary greatly between seasons, we calculated temporal statistics values by using multi-temporal images to obtain the distribution ranges of vegetation and snow areas, and obtained water body ranges by calculating the JRC monthly water history v1.3 dataset. Specifically, the water distribution data was adopted from the JRC monthly water history dataset v1.3 developed by the Joint Research Center of the European Commission, which had a resolution of 30 m and contained the spatiotemporal distribution of water surfaces and related statistics from 1984 to 2022 on a global scale. This study selected JRC data based on Landsat images from January 1, 2014 to January 1, 2016 to avoid uncertainties caused by short-term height dynamic changes of water (e.g., the difference between wet seasons and dry seasons). On this basis, we set the water probability threshold to 0.1, and then calculated the total number of observations and effective observations of water, as well as the number of observations with and without water within the effective observations. If the ratio was greater than the threshold value of 0.1, then the area was judged to be a water body. After obtaining all the water body information in the study area, a 60m buffer zone was constructed for it, so that the mudflat area around the water body was included in the water distribution data (Fig. 3). Vegetation distribution data were calculated using Sentinel-2 image data. Specifically, the 90% quantile of the NDVI value in the Sentinel-2 image data from June 23, 2015 to June 23, 2016 was selected (the maximum value was not taken because the extreme values were susceptible to noise interference), and compared to a threshold value of 0.25 (the usual value to distinguish whether there was vegetation cover), and if the 90% quantile of the NDVI value was greater than 0.25 then vegetation cover was considered to be present (Fig. 3).Snow distribution data is taken from Sentinel 2 pre-classification (snow, cloud, shadow, other) results. Specifically, the snow data from 2016 to 2022 in the Sentinel 2 product were selected. If the ratio of the number of observed snows to the number of effective observations was greater than the threshold value of 0.2 then snow distribution was considered to be present (Fig. 3). The extracted vegetation, snow, water and built-up areas were masked to reduce the images of irrelevant features, and the remaining features were the suspected areas of surface mining areas in the study area (Fig. 4a).

After removing irrelevant land types, the salt and pepper phenomenon in the image is obvious (mainly rural residential areas), causing visual interference. Therefore, we eliminated isolated pixels through morphological operations, and the remaining patches accounted for only 0.82% of the entire study area, which greatly reduced the workload (Fig. 4b). However, although most irrelevant land types have been deleted through masking and morphological operations, the remaining area still reached about 1088 km^2, and the distribution was scattered and the area span was large, which made it costly and difficult to identify all the mines using traditional field trekking methods. To fill the gap, this study, based on the

above-mentioned work, referred to the mine interpretation markers to interpret the map spots, and carried out direct observation and boundary outlining of remote sensing images for the remaining area (possible locations of surface mining areas) by visual interpretation method. This process was carried out in the Google Earth software, by referring to high-resolution satellite images around 2016, interpreting the remaining patterns, and delineating the boundaries of the mining area (Fig. 4c).

2.2.2 Bare surface percentage (BSP) time series and Mann-Kendall Test of surface mining areas

In order to monitor the rehabilitation of open pit mines, a dynamic time-series analysis of mine utilization characteristics is required. The greatest ecological impact of surface mining is the destruction of soil structure and thus vegetation growth (Xiao et al., 2023), and since one of the main efforts of mine rehabilitation is vegetation restoration and mountain restoration, the vegetation change characteristics of mine sites are commonly used to characterize the ecological changes in mine sites. Vegetation change characteristics can be characterized by various vegetation indices, such as NDVI, VARI, EVI, etc. Among them, numerous studies have confirmed that NDVI is a competent indicator for monitoring the vegetation in mining areas (Karan et al., 2016; Li et al., 2015; Yang et al., 2018). Therefore, in this study, by extracting the NDVI of the vegetation growth season in the mining areas, it is judged whether the mining area was rehabilitated based on whether the bare ground area has decreased, and on this bases, the Bare Surface Percentage (BSP) was constructed: if NDVI in the vegetation growth season was less than the threshold value 0.4, the area is determined to be in a bare ground state, and then the bare land ratio (BSP) of each mining area is obtained.

The formula for calculating the Bare Surface Percentage is as follows:

$$BSP_t = \frac{\mathrm{S_{bt}}}{\mathrm{S_t}} \times 100\backslash\% \ 1$$

Where: BSP_t represents the proportion of bare surface in year t, S_{bs} represents the area of bare surface in year t for a single mine site, S_t represents the total area of a single mine site in year t, and the ratio of the two is the proportion of bare surface in a single mine site. The BSP time series from 2016 to 2022 is constructed for each mine site, which can reflect the restoration situation and its trend to a certain extent.

To further determine the utilization characteristics and restoration of individual mines, we apply the Mann-Kendall Test (or MK test) to the BSP time series of each mine, which determines whether it has a monotonic trend and whether the trend is statistically significant, thereby distinguishing abandoned from non-abandoned mines, and internally comparing the restoration of mines in different utilization status. Specifically, the Mann-Kendall Test returns the following parameters, as shown in Table 2:

Table 2
The parameters of Mann-Kendall Test

Parameter	Implication
Trend	Describe the trend (increasing, decreasing or no trend)
h	True (with trend) or False (without trend)
p	The significance level, generally taken as p < 0.05 is significant
z	Standardized test statistics, with positive (negative) values of z indicating an increase (decrease) in data over time
Tau	Kendall rank correlation coefficient, positive (negative) when the trend is increasing (decreasing)
s	Interrelationship statistics between two variables
var_s	The variance S
slope	Theil-Sen valuator to estimate the size of the monotonic trend
intercept	Intercept of the Kendall-Theil line in full-cycle unit time steps

Using the Trend parameter returned by the MK test, we classified all mine sites in the study area as abandoned (BSP time series monotonically decreasing) and non-abandoned (BSP time series monotonically increasing or no trend), the former representing the site ceased its original use and underwent some degree of restoration treatment, and the latter representing the site still in use or lacking effective restoration treatment.

Further, in order to visually characterize the overall dynamic and continuous treatment of the mining area from 2016–2022, and to compare the overall treatment of the upstream, midstream and downstream mining areas horizontally, we further investigated the Restoration Rate (RR) of the overall mining areas in each region. The specific calculation formula for Restoration Rate is as follows:

$$RR_{ij} = \frac{S_i - \mathrm{S_j}}{\mathrm{S_j}} \times 100\backslash\%\ 2$$

Where: RR_{ij} represents the Restoration Rate from year i to year j. S_i represents the bare surface area of all surface mining area in year i, and S_j represents the bare surface area of all surface mining area in year j. The difference between the two is the total area of bare surface reduction during this period, that is, the total area treated. Comparing the total treated area with the total area of bare surface area in the year i is the restoration rate from year i to year j. This ratio can specifically reflect the effect of restoration in the study area.

2.2.3 Remote sensed Ecological index in Mining areas (REM) time series

Since one of the direct purposes of mine site restoration is to improve the local environment, this study further constructs a remotely sensed ecological indicator for mine sites to characterize the local environment condition, so as to evaluate the effect of mine site restoration in a result-oriented manner. Ecological environment remote sensing technology provides necessary monitoring data for ecological restoration or land reclamation activities, and also provides a convenient supervision tool for relevant departments, which has important practical value and research significance. On the basis of this technology, many Remote Sensed Ecological Indicators (RSEI) have been developed. The traditional RSEI can be expressed as a function of four sub-indices, greenness index (VI), moisture index (WET), heat index (LST), and dryness index (NDBSI):

$$RSEI = f\ G\ W\ T\ D \quad (3)$$

Its remote sensing definition is:

$$RSEI = f\ VI\ Wet\ LST\ NDBSI \quad (4)$$

The above four indicators are constructed based on Landsat-7 ETM + remote sensing images. After calculating the four sub-indicators through different bands, each indicator is normalized, and their dimensions are unified between [0,1]. Then the principal component analysis is carried out to obtain the initial ecological index $RSEI_0$. In order to facilitate the measurement and comparison of indicators, $RSEI_0$ is also normalized to obtain the Remote Sensed Ecological Indicator whose final value is between [0,1]. The closer the value is to 1, the better the ecological condition of the site, and vice versa, the worse the condition (Xu, H. Q., 2013).

However, when oriented to mine scenarios, most comprehensive indices of environment remote sensing fail to effectively take into account the problem of differences between soil and bare rock in sparsely vegetated areas (geotechnical differences), as well as the problem of differences in ecological quality due to plant diversity in densely vegetated areas. The Vegetation-Impervious surface-Soil framework in Mining area (VIS-M) is often used in the ecological evaluation of mining areas, i.e., in the ecological monitoring and evaluation of the mining areas concerned, the geotechnical difference is a key evaluation index: if the surface has a certain soil content, it indicates that the local area has a certain ability to cultivate vegetation, otherwise it is difficult to cultivate. This key factor is discriminated by the division between soil and bare rock, which plays a decisive factor in the local environment. In addition, since geotechnical differences cannot be evaluated with the same quality as the rest of the indicators, they are reflected as separate multipliers in the formula of the ecological index, and only two values of 0 and 1 are taken, i.e., as long as the area is bare rock, the final remote sensing ecological index is 0, and vice versa, this factor does not affect the final result. Therefore, in this study, the Remote sensed Ecological index in Mining areas (REM) (Sun et al., 2022) was constructed for the mines in the study area based on the VIS-M framework in a similar way to the RSEI. The specific calculation formula is as follows.

$$REM = I_{imper} \times \ \alpha \times I_{wet} + \beta \times I_{veg} + \gamma \times I_{soil} \quad 5$$

Where: I_{imper} represents whether the study area is bare rock or impervious layer, if it is bare rock, the value is 0, and vice versa, the value is 1; I_{wet} represents the degree of wetness of vegetation or soil, the higher the value represents the higher the quality of aquatic ecosystem; I_{veg} represents the combination of vegetation coverage and plant diversity, the higher the value represents the higher the quality of vegetation ecosystem; I_{soil} represents the combination of bareness and flatness of soil, the higher the value, the higher the quality of soil ecosystem; α, β and γ are the weight coefficients of the three indices, which are assigned to a single index by the principal component analysis method. The higher the value, the better the effect of environment management in the area.

3. Results

3.1 Spatial distribution of surface mining areas in the Yangtze River Basin

After the "Mask irrelevant land class - Remove isolated pixels - Visual interpretation of mine boundaries" process, the distribution of mines within a 10 km range along the Yangtze River and its tributaries is shown in Fig. 5. Based on the image characteristics of open-pit mine patches, this study visually interpreted a total of 1,183 surface mining areas in the study area, of which 696 were located in the main stem, while the tributaries contained 82, 46, 199, 89, 44, 7, and 20 mines for the Gan River, Xiang River, Wu River, Han River, Jialing River, Min River, and Yalong River, respectively (Fig. 5). The total study area was 132,633 km^2, of which vegetation and water bodies were the largest land cover types, accounting for 118,243 km^2 and 33,112 km^2, respectively, with a combined area of 94.1% of the entire study area. The sum of all surface mining areas was 1,088.078 km^2, accounting for 0.82% of the total study area (Fig. 5c), which was the smallest land cover type in the study area.

After obtaining the locations and boundaries of the mining areas within 10 km of the Yangtze River and its tributaries, we further compared our results with the mining area boundaries in the global mining database by Maus and Xie (Fig. 6). Maus' product is produced by visual interpretation of Sentinel-2 data and other high-resolution images based on the SNL metal and mining database by experts from Bing and Google (Maus et al., 2020), using a 10 km buffer zone to delimit the mining area boundaries. Xie's product, on the other hand, is based on various sources such as government reports, industry journals, and annual reports from mining companies, allowing for more refined delineation of mine boundaries (Tang et al., 2021). In contrast, the method used in this study to extract mining area locations does not rely on various forms of databases or publications. Instead, it only relies on open-source remote sensing data and uses methods based on land cover masks and morphological operations to identify potential locations of open-pit mines, greatly reducing the workload of visual interpretation. As shown in Fig. 6, the mining area locations and boundaries extracted in this study are generally consistent with the other two products. Compared with Maus' results, our results delimit mining area boundaries that are closer to the

actual bare earth boundaries. Compared with Xie's results, our results can more accurately identify small mining areas without omissions.

3.2 The restoration rate of surface mining areas in the Yangtze River Basin

This study aimed to monitor the utilization status and restoration of mines within a 10 km radius of the Yangtze River and its tributaries. A Bare surface percentage (BSP) time series based on Sentinel-2 remote sensing imagery was established for each mining area. Furthermore, the Mann-Kendall test was used to determine if there was a monotonic trend and whether it was statistically significant for each mining area's BSP time series. According to the Mann-Kendall trend test, the surface bare soil ratio of 381 mine areas showed a significant decreasing trend from 2016 to 2022, indicating that they were abandoned mines. 584 mine areas showed no significant trend, while 218 showed an increasing trend. To highlight the differences between abandoned mines and other mines in the BSP time series, we created a separate plot for mines with a monotonic decreasing trend according to the MK test (abandoned mines) and compared their BSP time series to those of all mines (Fig. 7c). The x-axis of the BSP change boxplot represents the year (2016–2022) and different categories of mines (abandoned mines and all mines), while the y-axis represents the BSP values (0%-100%). The 14 boxplot bodies in the figure represent BSP values between 10% and 90%. As shown in Fig. 7c, when comparing the BSP time series of the two mine categories from 2016 to 2022, we found that the Bare Surface Percentage of abandoned mines decreased year by year, with the median decreasing from 98% in 2016 to 81% in 2022, while the BSP time series of all mines, as a whole, showed an increasing trend, indicating that non-abandoned mines were still damaging the land due to ongoing utilization or insufficient restoration measures, resulting in larger bare surface. It is worth noting that in the initial state in 2016, the average level of BSP for abandoned mines was significantly higher than that for all mines, indicating better surface conditions for the latter. However, this difference gradually narrowed and reversed by 2022, with the mean BSP level of abandoned mines being significantly lower than that of all mines. This indicates an alarming trend of an increasing bare surface in non-abandoned mines.

To quantitatively demonstrate the extent of bare surface reduction in each mining area and each year, we calculated the restoration rates for 638, 421, and 124 mining areas in the upstream, midstream, and downstream of the Yangtze River, respectively (Fig. 7d). However, the results were still unsatisfactory. In the box plot of restoration rate changes, the horizontal axis represents the year (2016–2022) and the mining area location (upstream, midstream, and downstream), while the vertical axis represents the restoration rate of mining areas. The 24 box regions in the figure represent the restoration rates of mining areas in each region, ranging from 10–90% for each year. Unfortunately, almost half of the mining areas in the upstream, midstream, and downstream showed negative restoration rates, indicating an increase in bare land area compared to 2016. Furthermore, there are differences in restoration rates among mining areas in different regions. The downstream region has significantly higher lower limits of restoration rates

due to its flat terrain and better soil and vegetation conditions. However, the average restoration rate of mining areas in the middle region decreased at a much faster rate, indicating that there are a large number of mining areas with increasing bare surface area each year.

(a) Distribution of all mines in the Yangtze River Basin, (b) Distribution of abandoned mines in the Yangtze River Basin, (c) Changes in the Bare Surface Percentage of abandoned mines and all mines over time, (d) Changes in the Restoration Rate of mines in the upstream, midstream and downstream of the Yangtze River over time.

3.3 The ecological situation of surface mining areas in the Yangtze River Basin

After calculating the REM for each mining area in each year using Eq. (5), this study further analyzed and plotted the REM for all mining areas (Fig. 8a), abandoned mining areas (Fig. 8b), and active mining areas (Fig. 8c) from 2016 to 2022 to analyze the overall management situation of the study area. In the boxplot of REM changes, the x-axis represents the year (2016–2022) and the y-axis represents the REM value (0-0.35). The main body of the boxplot represents the REM values between the first and third quartiles from 2016 to 2022 for different types of mining areas. From a holistic perspective (Fig. 8a), most of the REM values in the study area were distributed between 0 and 0.25 during the seven years. Based on the 2020 inflection point, the REM value can be divided into a slow increase phase before 2020 and a sharp decline phase after 2020. When focusing on the 381 abandoned mining areas (Fig. 8b), we found that their REM values steadily increased from 2016 to 2021, which is consistent with the trend of the annual decrease in the BSP time series. When considering the 218 active mining areas (Fig. 8c), we found that their REM values had been declining over the past seven years, indicating the undeniable negative impact of mining activities on the local environment. It is worth noting that the REM values of the 381 abandoned mining areas decreased in 2021–2022, which is contrary to the goal of mining restoration and management.

To further explore the reasons why the overall ecological situation of surface mining areas in the Yangtze River Basin first rose and then declined from 2016 to 2022, this study analyzed each mining areas' average I_{veg} (Fig. 9a) and I_{imper} (Fig. 9b) from 2016 to 2022. I_{veg} represents the combination of vegetation coverage and plant diversity, the higher the value represents the higher the quality of vegetation ecosystem. I_{imper} represents the character of the subsurface of each mining area, the more impervious surface, the closer to 0. I_{veg} shows a stable trend in 2016–2021 and a decline in 2022, while I_{imper} consists a slow increase phase before 2020 and a sharp decline phase after 2020. I_{veg} and I_{imper} reveal the intrinsic causes of REM changes in the study area: vegetation has decreased and impervious surface has increased. The reasons for this phenomenon are the following: first, on an economic level, some abandoned mines have been redeveloped after greening, leading to a decrease in I_{veg} and I_{imper}; second, on a social level, the impact of the COVID-19 has forced the interruption of restoration and management work in some abandoned mines, resulting in a deterioration of the environment; third, on a project level, there may be cases where restoration work has been halted after the acceptance of the

project in 2020, resulting in a lack of long-term effectiveness evaluation and monitoring for the ecological restoration of mining areas and leading to further degradation of the environment. Finally, from an engineering perspective, there may be one or several missing factors in the treatment process related to the water quality of the aquatic ecosystem, vegetation coverage and diversity, as well as land leveling, leading to an overall lack of comprehensive and holistic treatment of the study area.

To better examine the changes in ecological quality within a single mining area, we conducted a REM change map for Mining Site 31 in Jiujiang City, Jiangxi Province (Fig. 10). From the distribution of REM within the mining area, it can be seen that the remote sensing ecological indices of the entire area were generally between 0.05 and 0.3 over the 7-year period. The center of the mining area had the lowest REM compared to other areas, indicating that the central area was the main mining point, and the degree of surface damage and bareness was more severe compared to other areas. In terms of time series changes, the REM changes in Mining Site 31 were consistent with the overall characteristics of all mining areas (Fig. 8a), showing a slow increase in REM from 2016 to 2020 and a sharp decrease from 2020 to 2022. As shown in Fig. 9g, the REM level of Mining Site 31 in 2022 was lower than that in 2016, and the low-value aggregation area in the center of the mining area was larger than in 2016. Even some areas with REM values close to 0.3 in 2016 had decreased to nearly 0.05 in 2022, indicating that the ecological quality of the mining area was worse than in 2016.

4. Discussion

4.1 A more reliable system for surface mining identification and recovering effect monitoring

Surface mining has a significant impact on the ecology. It is not easy to replenish mineral resources quickly, and the process of restoring the damaged area after mining can last for several decades. Hence, scholars worldwide have focused on identifying mining areas and monitoring mining reclamation. Numerous studies have been conducted from diverse perspective, including the impact on soil microorganisms, vegetation cover, and ecological effects.

Most studies related to mining activities are conducted within a specific mining zone, while identifying the boundaries of the surface mining area can be difficult, and it usually relies on pre-existing databases. This paper presents a comprehensive and structured approach that reduce the research area systematically by utilizing masks and morphological operations, enabling rapid identification of surface mining areas and facilitating reclamation monitoring and ecological assessment, which relies on freely accessible remote sensing data. This process has several advantages: (1) since the spectral characteristics of vegetation, snow, and water bodies are significantly different from those of surface mining areas, these areas can be easily eliminated by applying a spectral index mask, which can rapidly and significantly reduce the extent of analysis without introducing significant human intervention, thereby

decreasing the workload and processing requirements; (2) by establishing BSP time series and utilizing the MK-test, we can not only accurately distinguish abandoned mines from mines in operation, but also visualize the rehabilitation status of each mine intuitively; (3) on the basis of the ordinary remote sensing ecological indicators, the REM is derived from the Vegetation-Impervious surface-Soil framework in Mining area (VIS-M), which is particularly suitable for appraising the ecological quality of the mining areas; (4) all subsequent procedures are executed on the GEE platform. The computing capacity of the cloud platform removes the necessity of downloading numerous remote sensing images, which facilitates the full utilization of long-term remote sensing sequences for spatial temporal change monitoring. This approach enables rapid and effective processing of data.

Comparison with the products of Maus and Xie shows that the procedure of surface mining identification has a higher degree of accuracy and the extracted mines have fewer omissions. The monitoring results regarding restoration conditions and eco-environmental status convincingly demonstrate the potential of the proposed technique for automated monitoring of mining reclamation. The whole algorithm is developed on the GEE platform, which significantly enhances operational efficiency and convenience for large-scale implementation. The crucial feature of this technique is the continuous narrowing of the research area through a customized procedure to determine mining sites when they are unknown. This approach facilitates subsequent monitoring of mining reclamation extents and the associated environment.

4.2 Policy implications

Ecological restoration and remediation of surface mining areas is one of the important measures to enhance the value of land resources utilization and reduce the negative impact on the environment. Countries and regions worldwide have implemented policies and engineering measures to restore and manage surface mining areas. As early as 1977, the United States promulgated the Surface Mining Control and Reclamation Act (SMCRA) to regulate the environmental impact of coal mining, requiring the submission of effective reclamation plans when applying for coal exploration permits (Kite, 1977). In 1989, China implemented the Land Reclamation Regulations, and land reclamation in mining areas gradually began to receive attention. In 2006, land reclamation was included in China's mining license acquisition and land approval process. These practices provide important institutional support for protecting the environment of mining areas.

However, the results of this study indicate that when carrying out the restoration of mine clusters at the macro-regional level, blindly and randomly conducting restoration projects can easily result in certain ecologically sensitive areas not receiving timely treatment, overall restoration being neglected, and the overall environment being difficult to thoroughly improve. Therefore, the priority of mine restoration is a factor worthy of consideration in mine restoration and management. Specifically, when planning for the initial mine restoration project, information from various aspects such as the natural and social conditions of the research area needs to be collected. Differences in natural factors such as elevation, terrain slope, rock and soil differences, distance from water sources, and climate conditions can lead to varying risks of secondary disasters under the same mining intensity. Differences in social factors such

as population density, distance from the mining area to residential areas, and distance from the mining area to roads can lead to different threats and impacts on local residents and the socio-economy under the same risk intensity. Finally, it is also necessary to consider the mining conditions of the mining area itself, the ore reserves, the distance between the mine and the market, and the cost-benefit ratio of mining. Undoubtedly, under the same conditions, mining areas with high mining costs and low or small ore reserves need to be prioritized for restoration from an economic perspective.

Additionally, this study found that during the implementation of the mine restoration projects from 2016 to 2022, more than half of the 1,183 mines monitored had an increase in bare land area, and the overall ecological quality of the mines experienced a drastic decline in 2021–2022. This contradicts the goals of the restoration projects and indicates that the mine restoration efforts are still confined to the construction phase, lacking adequate follow-up maintenance mechanisms after construction ends. Therefore, the central or local governments should strengthen timely and objective monitoring of the restoration status, establish a long-term utilization mechanism for the evaluation and monitoring of the effectiveness of mine restoration projects to avoid deterioration after restoration, and improve the efficiency and effectiveness of mine restoration management over a longer time scale.

4.3 Limitations and future work

In this study, an open-source remote sensing data-based framework was developed to extract the locations and boundaries of open-pit mining areas on a large scale. On the basis of spatial statistical analysis, a monitoring system for the restoration of open-pit mines and an environmental evaluation system were established. However, our proposed framework and system have several limitations. Firstly, although the method used to extract mining areas in this study does not require field surveys or dependence on additional databases, visual interpretation and some degree of manual effort is still necessary when delineating mining boundaries on the Google Earth Engine platform. Secondly, due to the spectral similarity between bare land and mining areas, it is difficult to accurately distinguish mining areas from bare land and mudflats. Lastly, due to the limitations of Sentinel-2 remote sensing image resolution, it is difficult to extract micro-mining areas (such as small private mining pits). However, in situations where the area of bare land in mining areas is small, restoration is relatively easy, and the impact on the local environment compared to other large mining areas can be negligible. Therefore, the influence on the calculation of surface bareness and remote sensing ecological index in this study is minimal.

In future research, we plan to introduce more diverse data sources to distinguish between mining areas and other land cover types, and to avoid the mixing of mining areas with bare land and tidal flats caused by the spectral similarity of these features. This will improve the accuracy of identifying surface mining areas and enable the establishment of a more precise monitoring and ecological assessment system for restoration efforts.

5. Conclusion

Surface mining, as a common behavior in modern society, has a significant impact on the ecology. Identifying the extents of numerous surface mining areas on a large scale, particularly when a database with spatial location is unavailable, presents a challenging issue. With the help of freely-accessible remote sensing data, the method proposed in this paper realizes the rapid identification of surface mining areas and its restoration status and ecological quality in the Yangtze River Economic Belt.

In the study area of 132633 km^2, 1088 km^2 surface mining area is identified, representing 0.82% of the total study area. Among all 1183 mining areas, 381 abandoned mining areas showed a significant decreasing trend in surface bareness ratio from 2016 to 2021, while 218 mining areas were categorized as active mining areas and 584 mining areas showed no significant trend. The median value of BSP of the abandoned mining areas decreased from 98% in 2016 to 81% in 2022, indicating a better vegetation recovery during this period. Further analysis with remote sensing imagery revealed that the overall REM of abandoned mining areas showed a stable increasing trend from 2016 to 2022, except for a decrease in the last year due to various reasons. In contrast, the REM of active mining areas decreased annually during this period, indicating an undeniable negative impact of mining on the local environment.

The presented method is quick, user-friendly, and scalable to identify surface mining areas and monitor reclamation extents and ecological quality on a broader range. Moreover, it can be employed to assess the effectiveness of land reclamation and ecological restoration, as well as for mining and reclamation decision-making based on fundamental data. The method can also be applied to monitor the mining reclamation process in analogous regions and scenarios worldwide.

Declarations

Data availability

Data will be made available on request.

Ethical Approval

Not applicable.

Consent to Participate

Not applicable.

Consent to Publish

Not applicable.

Author Contributions

Suchen Xu: methodology, software, and supervision. Kechao Wang: writing — original draft, software, methodology, and data collection. Wu Xiao: conceptualization, methodology, validation, formal analysis, and writing — review and editing. Tong Tong: writing — review and editing, methodology, and supervision. Hao Sun: writing — review and editing, methodology, and supervision. Chong Li: methodology and supervision. Suchen Xu and Kechao Wang contributed equally.

Funding

The research was supported by the National Nature Science Foundation of China, Approval No. 42071250, and the China Postdoctoral Science Foundation Funded Project, Approval No. 2021M702795.

Competing Interests

The authors have no relevant financial or non-financial interests to disclose.

References

1. Ahirwal J, Maiti SK (2016) Assessment of soil properties of different land uses generated due to surface coal mining activities in tropical Sal (Shorea robusta) forest, India. Catena 140, 155–163
2. Belgiu M, Drăguţ L (2016) Random forest in remote sensing: A review of applications and future directions. ISPRS J Photogramm Remote Sens 114:24–31
3. Copeland C, Resources, Division I (2012) Mountaintop mining: background on current controversies. Congressional Research Service
4. Demetriou D, Stillwell J, See L (2012) Land consolidation in Cyprus: why is an integrated planning and decision support system required? Land Use Policy 29:131–142
5. Du XD, Zhang XK, Jin XB (2018) Assessing the effectiveness of land consolidation for improving agricultural productivity in China. Land Use Policy 70:360–367
6. Gorelick N, Hancher M, Dixon M, Ilyushchenko S, Thau D, Moore R (2017) Google Earth Engine: Planetary-scale geospatial analysis for everyone. Remote Sens Environ 202:18–27
7. Han Y, Ke YH, Zhu LJ, Feng H, Zhang Q, Sun Z, Zhu L (2021) Tracking vegetation degradation and recovery in multiple mining areas in Beijing, China, based on time-series Landsat imagery. GIScience Remote Sens 58:1477–1496
8. He MN, Wang YQ, Tong YP, Zhao YL, Qiang XK, Song YG, Wang L, Song Y, Wang GD, He CX (2020) Evaluation of the environmental effects of intensive land consolidation: A field-based case study of the Chinese Loess Plateau. Land Use Policy 94:104523

9. Huang Y, Tian F, Wang YJ, Wang M, Hu ZL (2015) Effect of coal mining on vegetation disturbance and associated carbon loss. Environ Earth Sci 73:2329–2342
10. Karan SK, Samadder SR, Maiti SK (2016) Assessment of the capability of remote sensing and GIS techniques for monitoring reclamation success in coal mine degraded lands. J Environ Manage 182:272–283
11. Kite MS (1977) The Surface Mining Control and Reclamation Act of 1977: An Overview of Reclamation Requirements and Implementation. Land Water Rev 13:703
12. LaJeunesse Connette KJ, Connette G, Bernd A, Phyo P, Aung KH, Tun YL, Thein ZM, Horning N, Leimgruber P, Songer M (2016) Assessment of mining extent and expansion in Myanmar based on freely-available satellite imagery. Remote Sens 8:912
13. Lechner AM, Kassulke O, Unger C (2016) Spatial assessment of open cut coal mining progressive rehabilitation to support the monitoring of rehabilitation liabilities. Resour Policy 50:234–243
14. Li J, Zipper CE, Donovan PF, Wynne RH, Oliphant AJ (2015) Reconstructing disturbance history for an intensively mined region by time-series analysis of Landsat imagery. Environ Monit Assess 187:1–17
15. Li SC, Zhao YL, Xiao W, Yellishetty M, Yang DS (2022) Identifying ecosystem service bundles and the spatiotemporal characteristics of trade-offs and synergies in coal mining areas with a high groundwater table. Sci Total Environ 807:151036. https://doi.org/10.1016/j.scitotenv.2021.151036
16. Liang YC, Liu G, Ma DC, Wang FC, Zheng H (2013) Regional cooperation mechanism and sustainable livelihoods: A case study on paddy land conversion program (PLCP). Acta Ecol Sin 33:693–701
17. Maus V, Giljum S, Gutschlhofer J, da Silva DM, Probst M, Gass SLB, Luckeneder S, Lieber M, McCallum I (2020) Sci Data 7:289. https://doi.org/10.1038/s41597-020-00624-w. A global-scale data set of mining areas
18. Mitchell Waldrop M (2019) News feature: what are the limits of deep learning. Proc Natl Acad Sci 116:1074–1077
19. Mountrakis G, Im J, Ogole C (2011) Support vector machines in remote sensing: A review. ISPRS J Photogramm Remote Sens 66:247–259
20. Mukherjee J, Mukherjee, Jayanta, Chakravarty D, Aikat S (2019) A novel index to detect opencast coal mine areas from Landsat 8 OLI/TIRS. IEEE J Sel Top Appl Earth Obs Remote Sens 12:891–897
21. Murguía DI, Bringezu S (2016) Measuring the specific land requirements of large-scale metal mines for iron, bauxite, copper, gold and silver. Prog Ind Ecol Int J 10:264–285
22. Petropoulos GP, Partsinevelos P, Mitraka Z (2013) Change detection of surface mining activity and reclamation based on a machine learning approach of multi-temporal Landsat TM imagery. Geocarto Int 28:323–342
23. Ren H, Zhao YL, Xiao W, Zhang JY, Chen CF, Ding BL, Yang X (2022) Vegetation growth status as an early warning indicator for the spontaneous combustion disaster of coal waste dump after reclamation: An unmanned aerial vehicle remote sensing approach. J Environ Manage 317:115502

24. Singh P, Kikon N, Verma P (2017) Impact of land use change and urbanization on urban heat island in Lucknow city, Central India. A remote sensing based estimate. Sustain Cities Soc 32:100–114
25. Sklenicka P, Šímová P, Hrdinová K, Salek M (2014) Changing rural landscapes along the border of Austria and the Czech Republic between 1952 and 2009: Roles of political, socioeconomic and environmental factors. Appl Geogr 47:89–98
26. Sun H, Hu JQ, Jiang JB, Zhao YL, Sun WB, Cui XM (2022) REM: a remote sensing ecological index of mining areas considering plant diversity and rock-soil difference. J China Coal Soc. https://doi.org/10.13225/j.cnki.jccs.XR21.2076
27. Tamiminia H, Salehi B, Mahdianpari M, Quackenbush L, Adeli S, Brisco B (2020) Google Earth Engine for geo-big data applications: A meta-analysis and systematic review. ISPRS J Photogramm Remote Sens 164:152–170
28. Tang L, Tim T, Xie W, Yang HP, Shi JS, Z.M (2021) A global-scale spatial assessment and geodatabase of mine areas. Glob Planet Change 204:103578. https://doi.org/10.1016/j.gloplacha.2021.103578
29. Vasuki Y, Yu L, Holden E-J, Kovesi P, Wedge D, Grigg AH (2019) The spatial-temporal patterns of land cover changes due to mining activities in the Darling Range, Western Australia: A Visual Analytics Approach. Ore Geol Rev 108:23–32
30. Venkateswarlu K, Nirola R, Kuppusamy S, Thavamani P, Naidu R, Megharaj M (2016) Abandoned metalliferous mines: ecological impacts and potential approaches for reclamation. Rev Environ Sci Biotechnol 15:327–354
31. Wang YF, Li XJ, Li FQ, Wang Y (2019) Identification of typical disturbance trajectouy in coal mining sbsidence area based on multi-tenporal remote sensing images. Acta Geol Sinca 93:301–309
32. Werner TT, Bebbington A, Gregory G (2019) Assessing impacts of mining: Recent contributions from GIS and remote sensing. Extr Ind Soc 6:993–1012
33. Werner TT, Mudd GM, Schipper AM, Huijbregts MA, Taneja L, Northey SA (2020) Global-scale remote sensing of mine areas and analysis of factors explaining their extent. Glob Environ Change 60:102007
34. Wong MH (2003) Ecological restoration of mine degraded soils, with emphasis on metal contaminated soils. Chemosphere 50:775–780
35. Wu QH, Liu K, Song CQ, Wang JD, Ke LH, Ma RH, Zhang WS, Pan H, Deng XY (2018) Remote sensing detection of vegetation and landform damages by coal mining on the Tibetan Plateau. Sustainability 10, 3851
36. Xiao W, Chen WQ, Deng XY (2021) Coupling and coordination of coal mining intensity and social-ecological resilience in China. Ecol Indic 131:108167
37. Xiao W, Deng XY, He TT, Guo JW (2023) Earth Engine J Environ Manage 327:116920. https://doi.org/10.1016/j.jenvman.2022.116920. Using POI and time series Landsat data to identify and rebuilt surface mining, vegetation disturbance and land reclamation process based on Google

38. Xiao W, Ren H, Sui T, Zhang HY, Zhao YL, Hu ZQ (2022) A drone-and field-based investigation of the land degradation and soil erosion at an opencast coal mine dump after 5 years' evolution of natural processes. Int J Coal Sci Technol 9:42
39. Xiao W, Zhang WK, Ye YM, Lv XJ, Yang WF (2020) Is underground coal mining causing land degradation and significantly damaging ecosystems in semi-arid areas? A study from an Ecological Capital perspective. Land Degrad Dev 31:1969–1989
40. Xing ZG, Peng SP, He YL, Chong S, Feng FS, Yu P, She CC, Xu DJ (2018) Hydrogeological changes caused by opencast coal mining in steppe zone: a case study of Shengli 1 open-pit coal mine. Desalin Water Treat 121:126–133
41. Xiong Y, Xu WH, Lu N, Huang SD, Wu C, Wang LG, Dai F, Kou WL (2021) Assessment of spatial–temporal changes of ecological environment quality based on RSEI and GEE: A case study in Erhai Lake Basin, Yunnan province, China. Ecol Indic 125:107518
42. Xu HQ (2013) A remote sensing urban ecological index and its application. Acta Ecol Sin 33:7853–7862
43. Xu HQ, Wang MY, Shi TT, Guan HD, Fang CY, Lin ZL (2018) Prediction of ecological effects of potential population and impervious surface increases using a remote sensing based ecological index (RSEI). Ecol Indic 93:730–740
44. Xu HQ, Wang YF, Guan HD, Shi TT, Hu XS (2019) Detecting ecological changes with a remote sensing based ecological index (RSEI) produced time series and change vector analysis. Remote Sens 11:2345
45. Xu JX, Zhao H, Yin PC, Jia D, Li G (2018) Remote sensing classification method of vegetation dynamics based on time series Landsat image: a case of opencast mining area in China. EURASIP J. Image Video Process. 2018, 1–10
46. Yang YJ, Erskine PD, Lechner AM, Mulligan D, Zhang SL, Wang ZY (2018) Detecting the dynamics of vegetation disturbance and recovery in surface mining area via Landsat imagery and LandTrendr algorithm. J Clean Prod 178:353–362
47. Yu L, Xu YD, Xue YM, Li XC, Cheng YQ, Liu XX, Porwal A, Holden E-J, Yang J, Gong P (2018) Monitoring surface mining belts using multiple remote sensing datasets: A global perspective. Ore Geol Rev 101:675–687
48. Zarch MAA, Sivakumar B, Sharma A (2015) Droughts in a warming climate: A global assessment of Standardized precipitation index (SPI) and Reconnaissance drought index (RDI). J Hydrol 526:183–195
49. Zhang MX, He TT, Li GY, Xiao W, Song HP, Lu DB, Wu CF (2021) Continuous Detection of Surface-Mining Footprint in Copper Mine Using Google Earth Engine. Remote Sens 13:4273. https://doi.org/10.3390/rs13214273
50. Zhang MX, He TT, Wu CF, Li GY (2022) The Spatiotemporal Changes in Ecological–Environmental Quality Caused by Farmland Consolidation Using Google Earth Engine: A Case Study from Liaoning Province in China. Remote Sens 14:3646

51. Zhu XX, Tuia D, Mou LC, Xia GS, Zhang LP, Xu F, Fraundorfer F (2017) Deep learning in remote sensing: A comprehensive review and list of resources. IEEE Geosci Remote Sens Mag 5:8–36
52. Zhu Z, Wulder MA, Roy DP, Woodcock CE, Hansen MC, Radeloff VC, Healey SP, Schaaf C, Hostert P, Strobl P (2019) Benefits of the free and open Landsat data policy. Remote Sens Environ 224:382–385

Figures

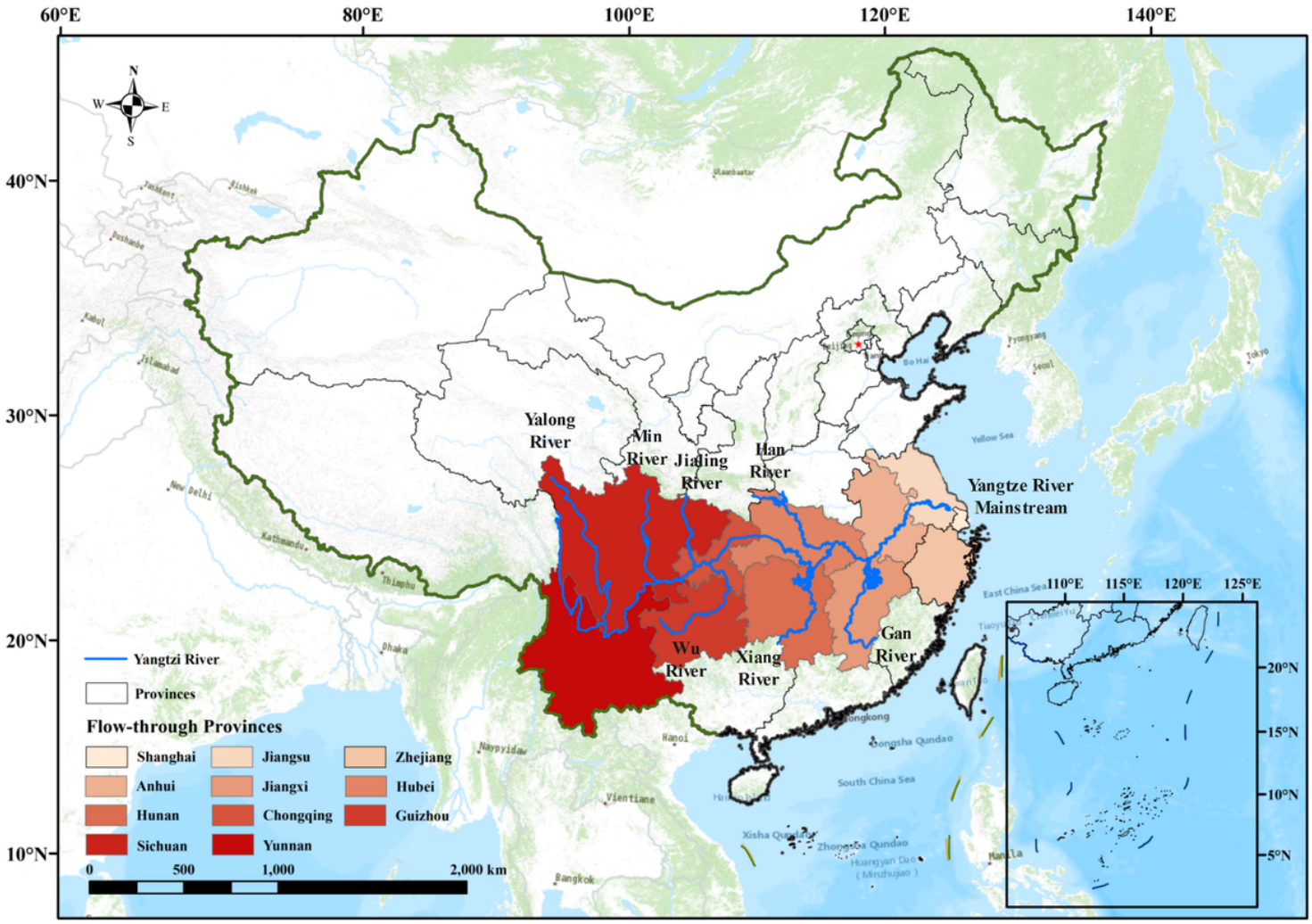

Figure 1

Location of Yangtze River and Yangtze River Economic Belt.

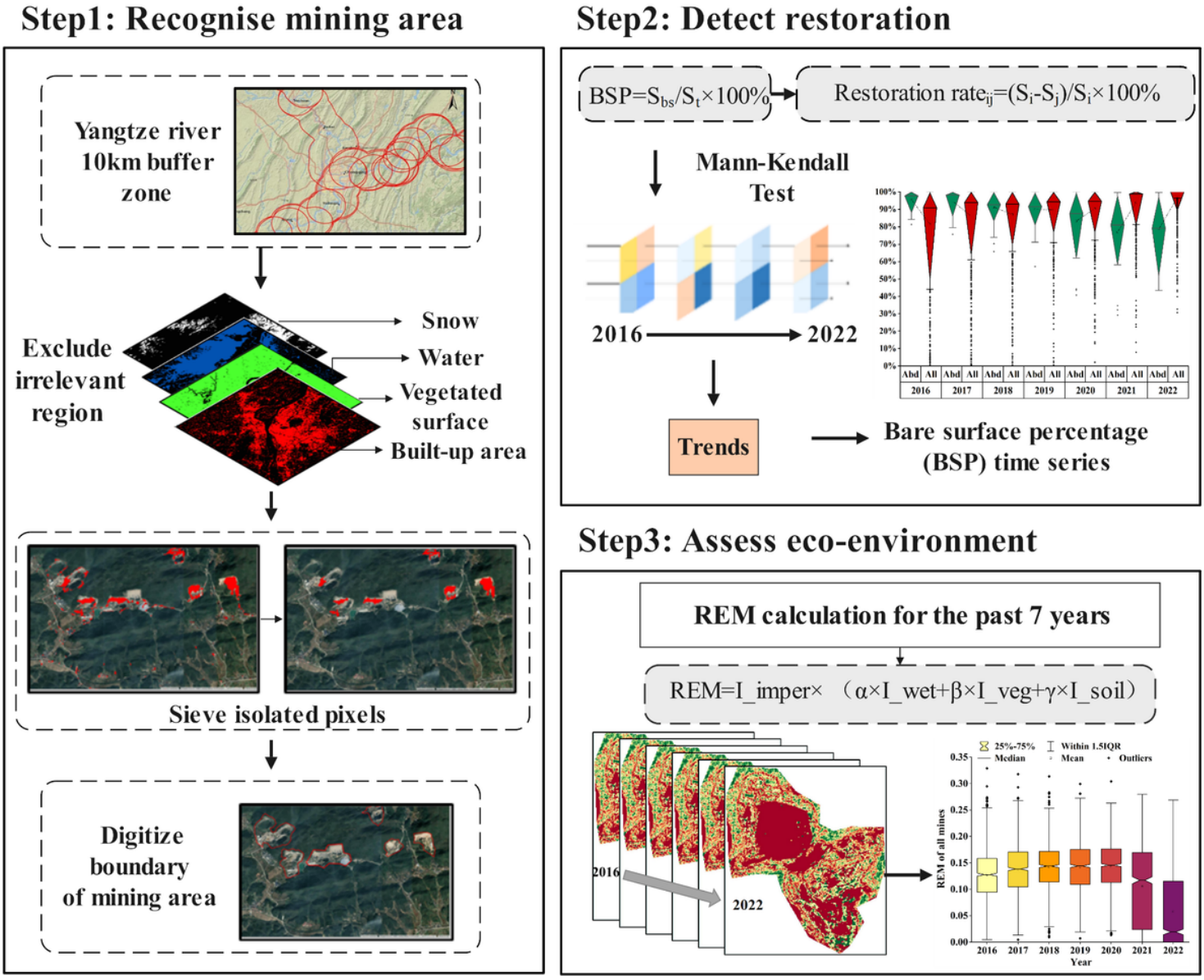

Figure 2

Technical framework

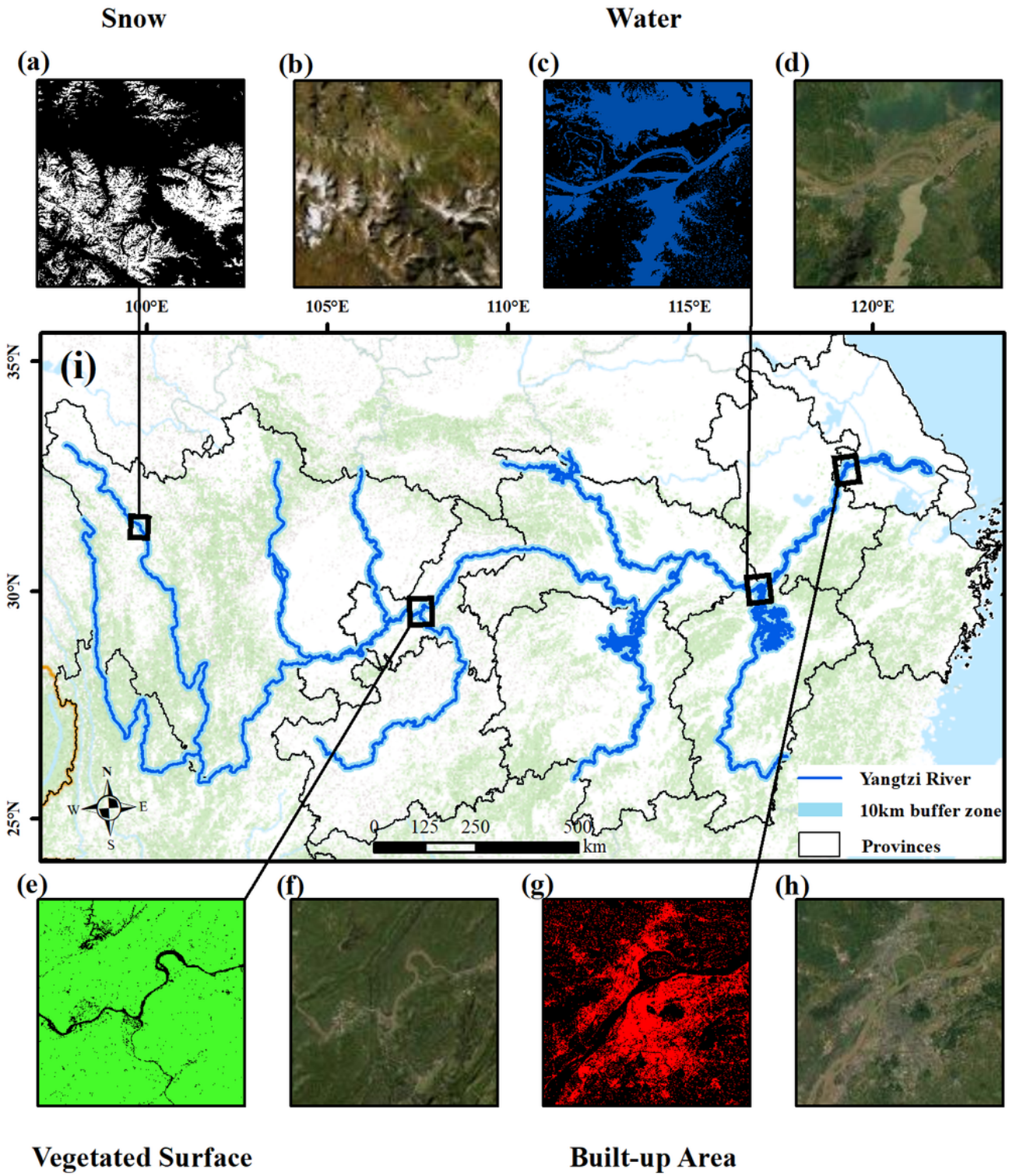

Figure 3

Yangtze River and its 10 km buffer zone and four feature types

(a) snow distribution area in Sentinel-2 images; (b) snow distribution area in Google Earth images; (c) water distribution area in Sentinel-2 images; (d) water distribution area in Google Earth images; (e) vegetation distribution area in Sentinel-2 images; (f) vegetation distribution area in Google Earth images;

(g) built-up area distribution area in Sentinel-2 images; (h) built-up area distribution area in Google Earth images.

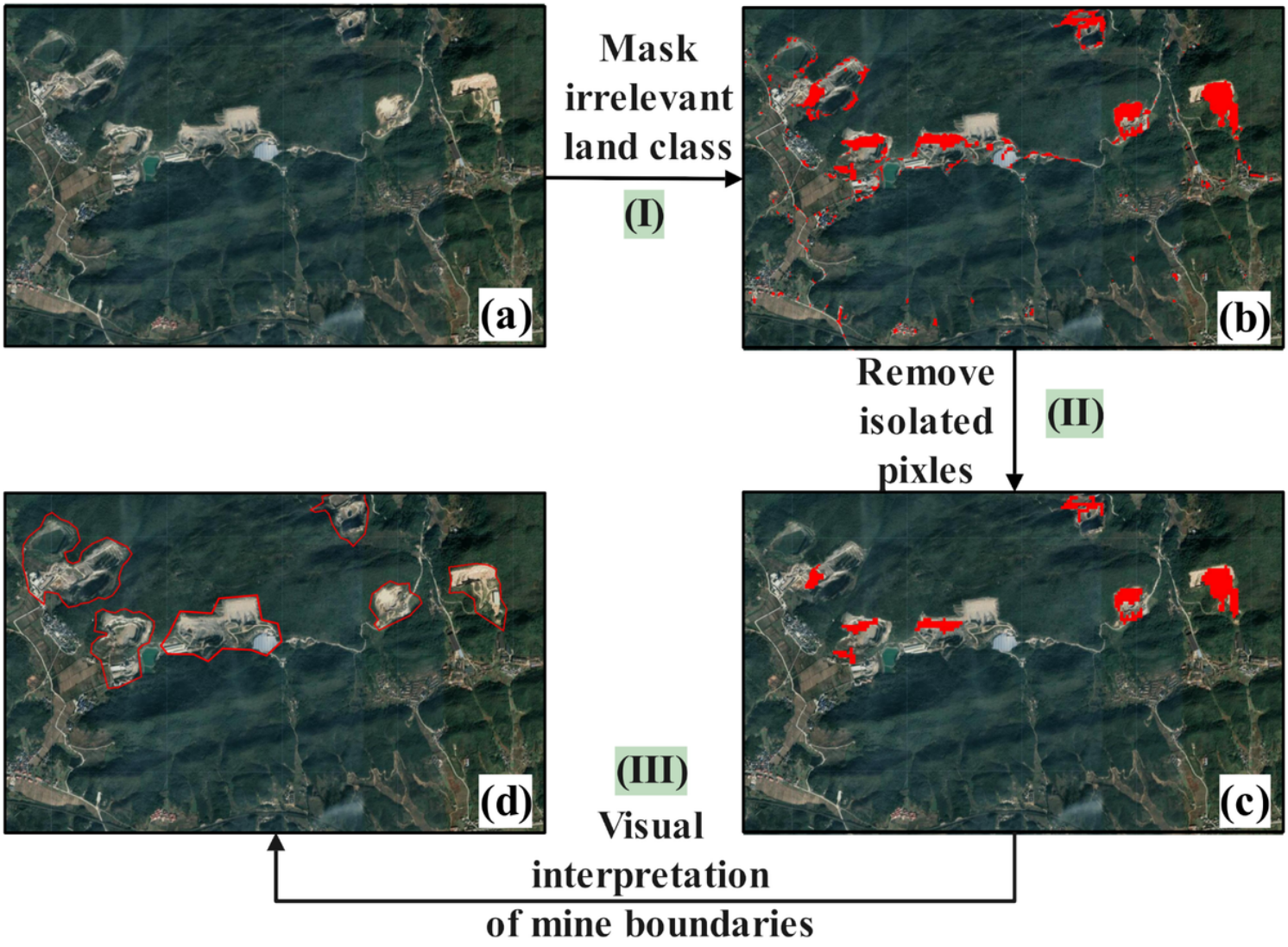

Figure 4

Remote sensing identification and digital workflow of open pit mine.

(a) The original image of the study area; (b) Extraction and masking of irrelevant terrain types; (c) Morphological operations to remove isolated pixels; (d) Visual interpretation and digitization of the mine boundary

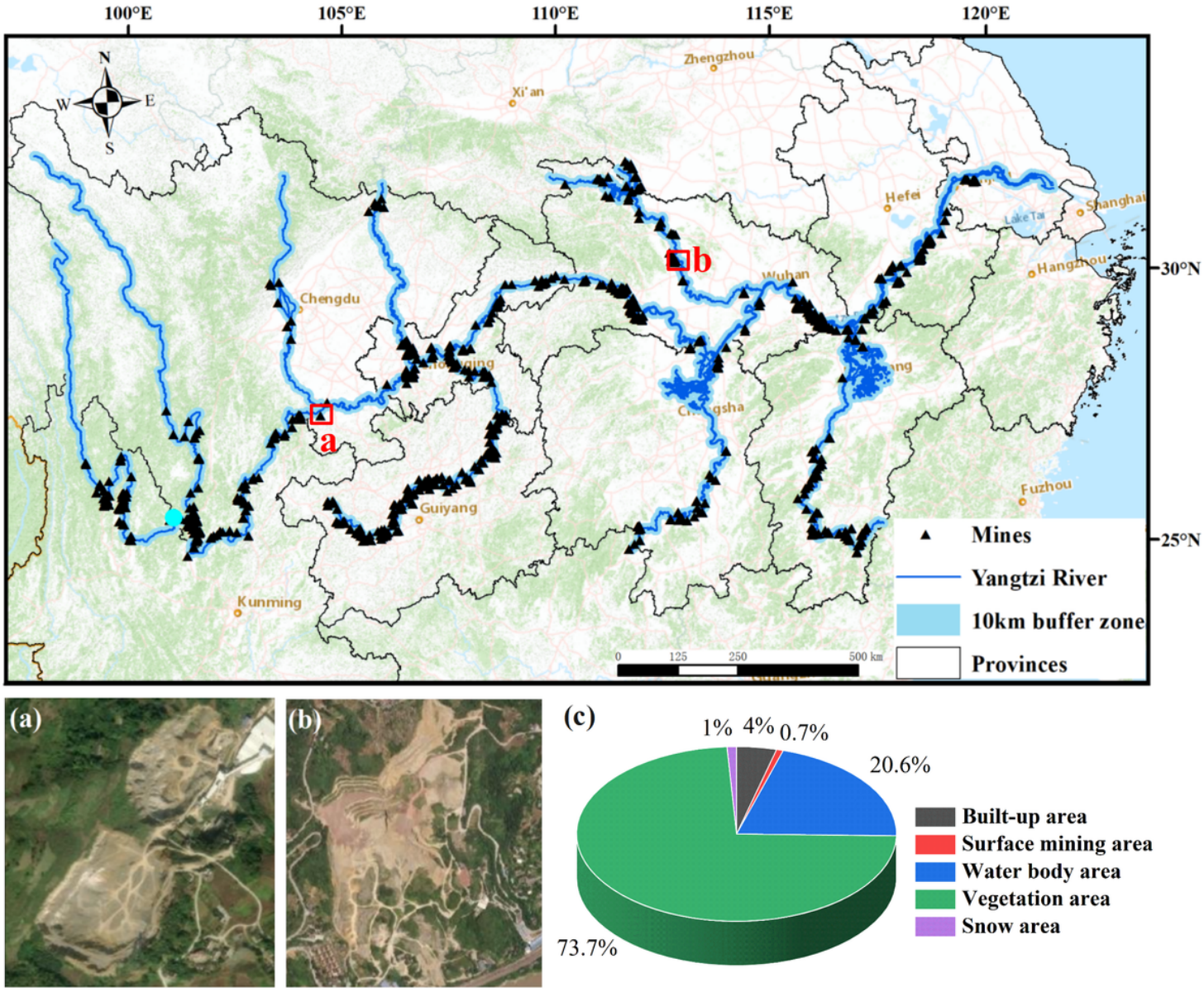

Figure 5

Distribution of mines within 10 km along the main and tributary of the Yangtze River, Google image and the proportion of each type of area in the study area

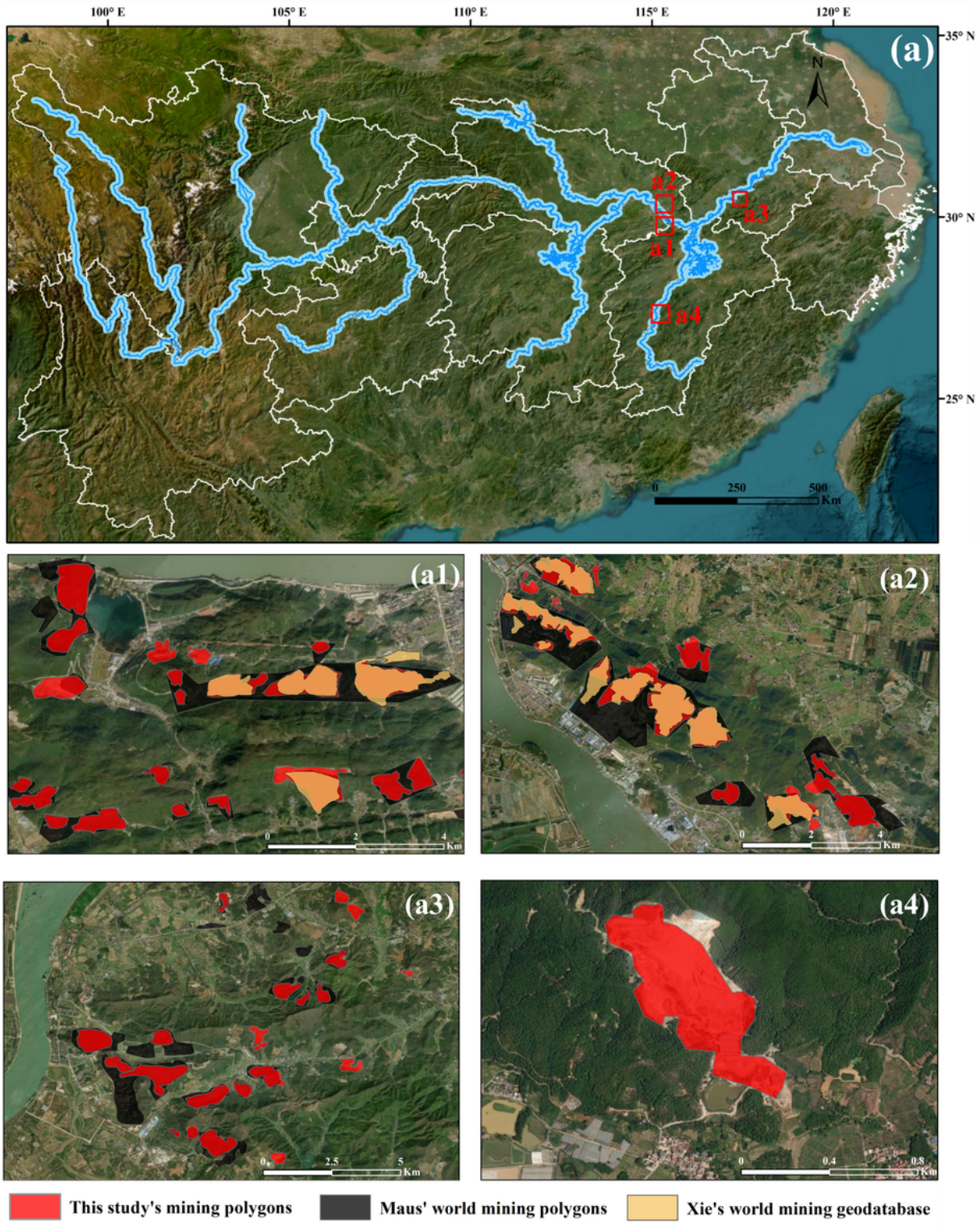

Figure 6

Comparison with two global mining monitoring products (Maus' and Xie's products) within the study area.

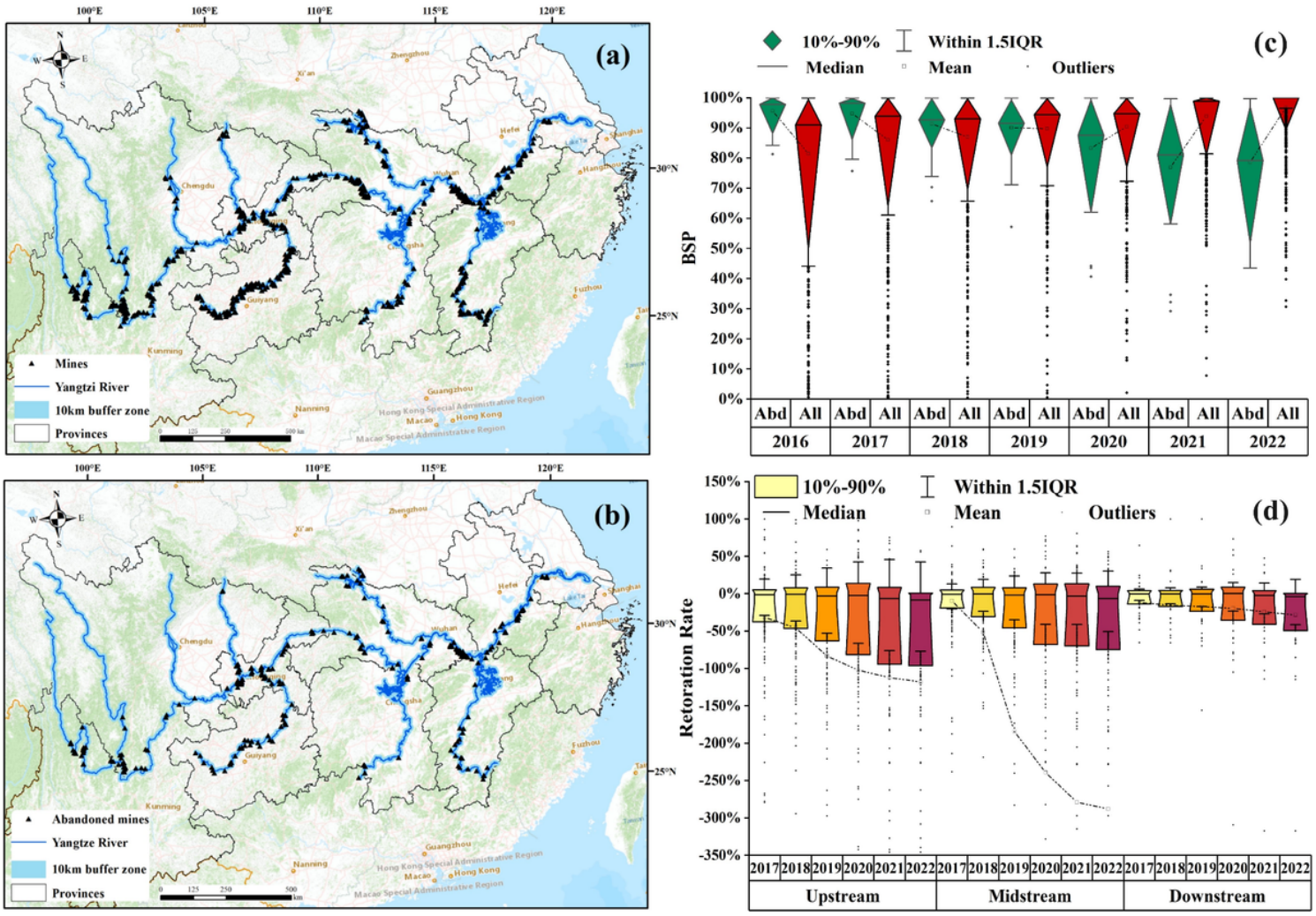

Figure 7

Restoration and management of mining areas in the Yangtze River Basin.

(a) Distribution of all mines in the Yangtze River Basin, (b) Distribution of abandoned mines in the Yangtze River Basin, (c) Changes in the Bare Surface Percentage of abandoned mines and all mines over time, (d) Changes in the Restoration Rate of mines in the upstream, midstream and downstream of the Yangtze River over time.

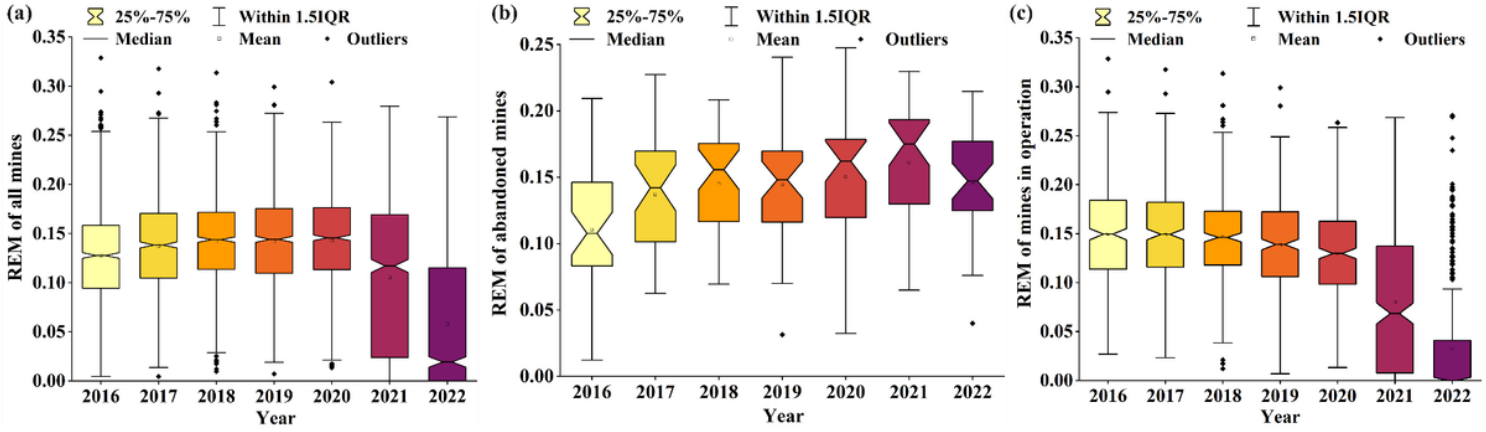

Figure 8

REM changes over time.

(a)REM changes for all mines, (b) REM changes for abandoned mines, (c) REM changes for mines in operation.

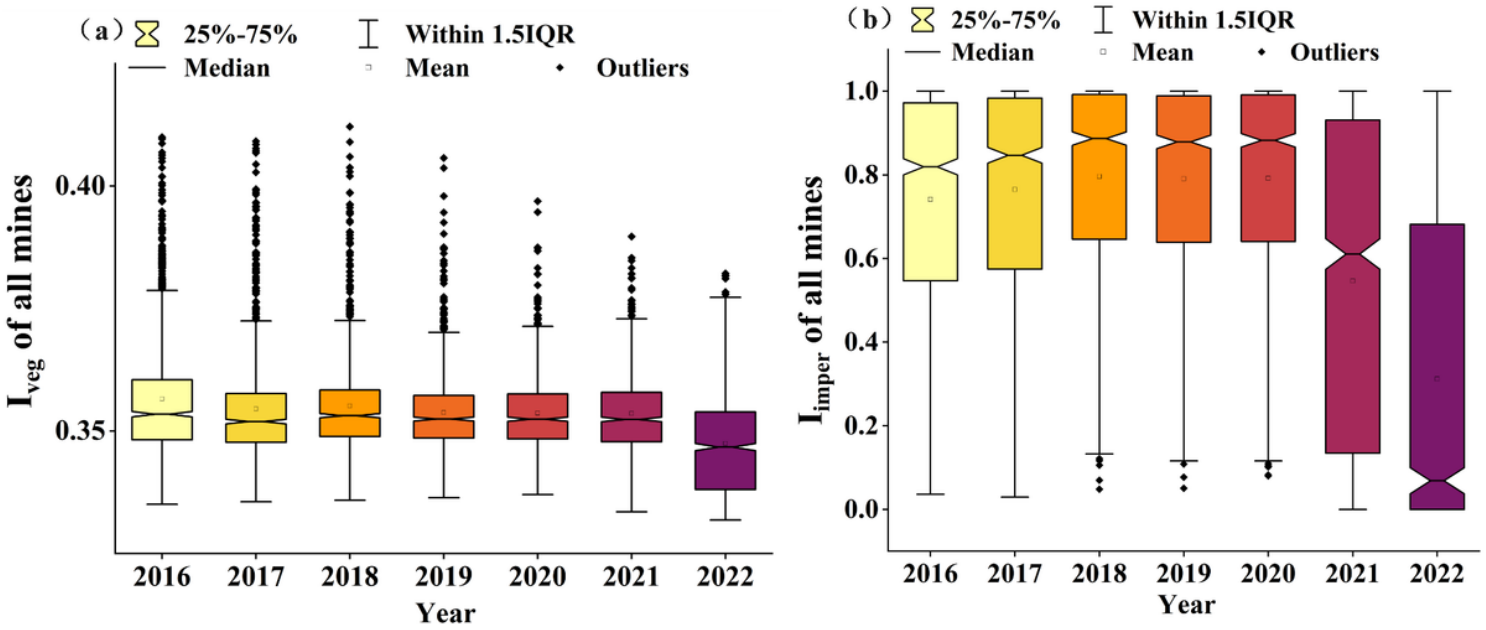

Figure 9

I_{veg} and I_{imper} changes over time.

(a) I_{veg} changes for all mines, (b) I_{imper} changes for abandoned mines.

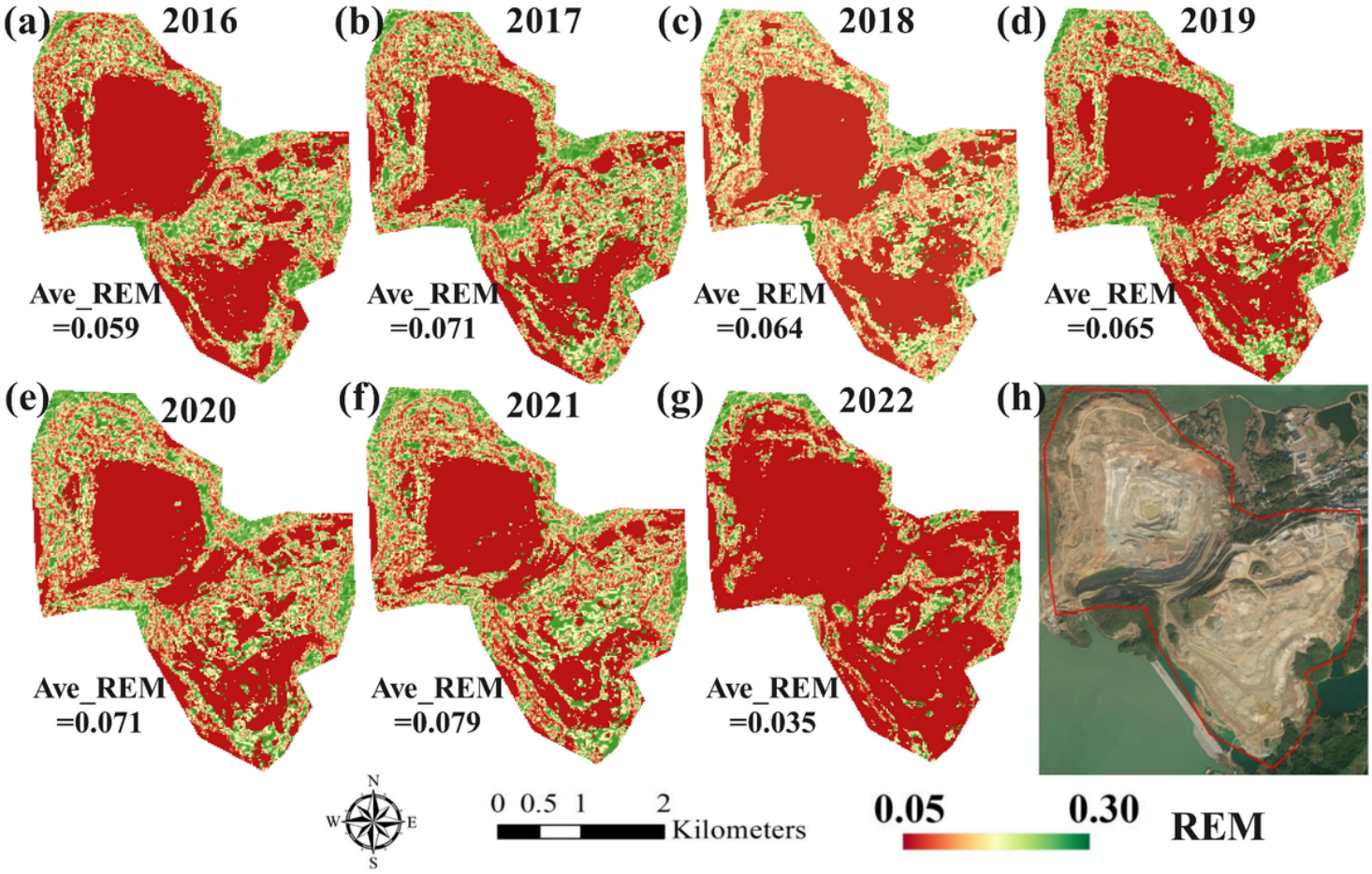

Figure 10

Annual REM of No. 31 Mining Area in Jiujiang City, Jiangxi Province